Advancing soil moisture climate records through the integration of SMOS observations

van der Schalie, R.

2017

document version
Publisher's PDF, also known as Version of record

5 Evaluation of the SMOS and AMSR-E LPRM soil moisture data sets by comparison against two alternative merging approaches

This chapter is on the effects of different frequencies and merging approaches on the quality of soil moisture data sets. Three different merging approaches are evaluated that use AMSR-E and SMOS observations to create a long term dataset. Both the skill of the soil moisture as the consistency between the data from the two sensors are tested. Soil moisture based on the active microwave sensor ASCAT is also included to better put the results in perspective. Chapter 5 is based on the following publication:

Van der Schalie, R., De Jeu, R.A.M., Rodríguez-Fernández, N.J., Al-Yaari, A., Kerr, Y.H., Wigneron, J.P., Parinussa, R.M., and Drusch, M.. Evaluation of three different data fusion approaches for the development of a soil moisture climate record based on passive microwave satellite sensors. IN REVIEW.

5.1 Introduction

Long term, consistent soil moisture records are essential to improve our understanding of the impact of climate change, as already demonstrated in many research studies (e.g. see Dorigo et al, 2016 for a comprehensive overview). In 2010, the importance of soil moisture was recognized by the Global Climate Observation System (GCOS) which labeled this important variable as an Essential Climate Variable (ECV) (GCOS, 2010).

Direct measurements of soil moisture can be done with in situ sensor networks, but the current coverage is sparse and unequally distributed worldwide. Secondly, soil moisture from in situ sensors generally have a small spatial support which makes the use of in situ networks unsuitable for providing reliable global soil moisture climate records. Problems with continuity, sensor characteristics and non-uniform data processing make consistency also a big issue, however an initiative like the International Soil Moisture Network initiative (ISMN, Dorigo et al., 2011 & Dorigo et al. 2013) aims to improve this. Satellite observations from both active as passive microwave sensors are able to fill this gap, as the dielectric properties of the soil, especially at lower frequencies, can be directly related to the water content of the top layer of the soil (Schmugge et al., 1974).

Especially in the last two decades, an increased effort has been made to develop algorithms that can derive soil moisture from both passive and active microwave observations (Owe et al., 2001; Wagner et al., 1999; Wigneron et al., 1995; Njoku et al., 2003; Jackson, 1993), for which Observations from the Advanced Microwave Scanning Radiometer - Earth Observing System (AMSR-E) often formed the base for the development (i.e. C- and X-band frequencies, Mladenova et al. 2014). For active microwave based soil moisture retrievals, observations from ESA's two European Remote Sensing (ERS) satellites, ERS-1 and –2, provided researchers with a source of input (Wagner et al., 1999). Recently, two soil moisture dedicated missions have been launched, the Soil Moisture and Ocean Salinity mission in 2009 (SMOS, Kerr et al., 2010) and the Soil Moisture Active Passive

mission in 2015 (SMAP, Entekhabi et al., 2010), which observe the Earth in the L-band frequency (1.4 GHz). Theoretically this is the most optimal frequency for surface soil moisture sensing due to its increased sensing depth (approximately the first 5 cm instead of the first 2 cm from C- and X-band), decreased sensitivity to vegetation and higher sensitivity to soil moisture dynamics as compared to the higher frequencies. This gave way to the development of L-band specific algorithms (Wigneron et al., 2007; Kerr et al., 2012; Entekhabi et al., 2010; Konings et al., 2016; Van der Schalie et al., 2016).

In 2010, ESA initiated a project with the goal to develop a consistent long term dataset of soil moisture derived from a wide range of active and passive microwave sensors (http://www.esa-soilmoisture-cci.org, Dorigo et al., IN REVIEW). The work presented here is part of ESA's the Climate Change Initiative (CCI) program. The CCI soil moisture dataset (ESA-CCI-SM) is currently the most popular ESA CCI product with over 3200 registered users. The ESA-CCI-SM consists of a merger between active and passive soil moisture retrievals following the baseline methodology of Liu et al. (2011 & 2012), which was recently further advanced (Chung et al. 2016). This merging of active and passive is based on the complementary of the two data sources, with passive soil moisture retrievals performing better over sparsely vegetated areas, and active sensors performing better over more densely vegetated areas (De Jeu et al., 2008; Dorigo et al., 2010).

Building a consistent long term soil moisture dataset is not straight forward, especially due to large differences in satellite sensor characteristics and retrieval algorithms. Therefore, several alternative merging approaches are currently under development (Al-Yaari et al., 2015; Rodriguez-Fernandez et al., 2016; Van der Schalie et al., 2017). It is currently still unclear what the effect is of using different merging approaches, and how this reflects back on the quality of the datasets. This study aims to provide insight in this question by evaluating three different merging strategies.

With the arrival of the L-band missions, these merging approaches have an increased focus on the integration of L-band based soil moisture retrievals in a climate record. They already have been applied to satellite observations from both AMSR-E (2003 – 2011) and SMOS (2010-onwards). The first fusion method is based on a global neural network approach (NN, Rodriguez-Fernandez et al., 2015 & 2016), which trains AMSR-E brightness temperature observations from its multiple frequencies to match the official SMOS soil moisture product, SMOS Level 3 (L3), and then applies the NN retrospectively to the AMSR-E period. The second fusion method also uses SMOS L3 soil moisture as the training dataset for AMSR-E observations, and the training is based on local regressions (REG, Wigneron et al., 2004; Al-Yaari et al., 2015) and applying regression coefficients retrospectively to the AMSR-E period. The third approach uses an refined version of the Land Parameter Retrieval Model (LPRM, Owe et al., 2008; Van der Schalie et al., 2017), which is the current baseline algorithm for passive microwave component in the ESA-CCI-SM. The LPRM was further developed for the application to SMOS L-band observations (Van der Schalie et al., 2015 & 2016). To better put the results in perspective of the existing CCI merging, soil moisture retrievals based on observations from the Advanced Scatterometer (ASCAT, Naeimi et al., 2009) are also included in the evaluation. The ASCAT soil moisture reflects the active counterpart from the year 2006 onwards as used in the ESA-CCI-SM and is retrieved using the Change Detection Algorithm (CDA, Wagner et al., 1999). This will provide the ESA-CCI-SM data users the opportunity to better understand the pros and cons of these different sensors and merging strategies.

A first indication of the quality of the these merging strategies was provided by Rodriguez-Fernandez et al. (2016), where the three different AMSR-E datasets (NN, REG and LPRM) were compared against in situ data and modelled data from NASA's Modern-Era Retrospective analysis for Research and Applications - Land (MERRA-Land, Reichle et al., 2011) and from European Centre for Medium-Range Weather Forecasts its ERA-Interim/Land (Balsamo et al., 2015). Van der Schalie et al. (2016) presented an extensive comparison between the two SMOS datasets (L3 and LPRM)

against in situ measurements from the ISMN. However, as discussed earlier, the use of ground observations has its shortcomings. Models on the other hand, do have global coverage, but contain unique error characteristics and the results are therefore difficult to interpret. In order to overcome this problem, several methods have been developed that are better able to quantify the skill of soil moisture datasets. One of these is the so-called R_{value} verification technique (Crow et al., 2010; Parinussa et al., 2011), which is a large scale precipitation based validation technique that is a robust representation of (anomaly) correlation based skill in satellite soil moisture retrievals. Another method is the Triple Collocation Analysis (TCA, Scipal et al., 2008; Dorigo et al., 2010; Draper 2013), which uses three collocated soil moisture datasets in order to estimate the root mean square error (*rmse*), in absence of a dataset that can be used as the absolute truth at the global scale.

In this study, the different merging strategies are evaluated focusing on consistency between the merged datasets in the first step, and then defining the skill of the individual datasets in the next steps. The four steps are: (1) An inter-comparison exercise between the AMSR-E and SMOS fusion approaches, i.e. LPRM/NN/REG, to check the consistency between the datasets in their overlapping period, the skills of the SMOS, AMSR-E and ASCAT soil moisture anomalies were determined through (2) the R_{value} technique, and (3) the TCA. In a final exercise, (4) we explicitly focus on two regions that have strong land-atmosphere coupling, the Sahel and the central Great Plains of northern America (Koster et al., 2006; Seneviratne et al., 2010; Miralles et al., 2012). These regions were analyzed in more details as soil moisture plays and important role here from a climate perspective, as changes in soil moisture can directly affect the energy fluxes and weather patterns over these regions. This will provide more insight in the use of soil moisture records for climate research purposes.

5.2 Data

5.2.1 AMSR-E

The AMSR-E is a sensor on the Aqua satellite, which is a joint collaboration of the Japan Aerospace Exploration Agency (JAXA) and NASA. AMSR-E is a passive microwave radiometer that was in operation between 2002 and 2011, and measured the Earth's emission in six different frequencies (6.9 – 89.0 GHz), in both horizontal and vertical polarization. The mean spatial resolution of the radiometer observations decreases from 56 to 5.4 km with increasing frequency. Before the arrival of the new generation L-band missions, AMSR-E was an important data source for the development of passive microwave soil moisture retrieval algorithms (Mladenova et al., 2014). Although the C- and X-band (6.9 and 10.7 GHz) observations are theoretically not as optimal for soil moisture retrievals as L-band, this downside can potentially be balanced out with higher sensor accuracies. Secondly, the multi-frequency observations from AMSR-E give a unique ability to switch between frequencies when the frequency is disturbed by artificial noise which is often named as Radio Frequency Interference (RFI) (Li et al., 2004; De Nijs et al., 2015; Parinussa et al., 2017), and to simultaneously retrieve the soil temperature from higher frequencies (e.g. from 36.5 GHz observations, Holmes et al., 2009; Parinussa et al., 2011). Three different soil moisture datasets derived from AMSR-E observations are used in this study, the AMSR-E NN, AMSR-E REG and AMSR-E LPRM. Only observations from the descending overpasses of AMSR-E (01.30 AM) are used, as it generally results in higher quality retrievals (De Jeu et al, 2008; Parinussa et al., 2011; Parinussa et al., 2017). The AMSR-E based datasets were provided in a 25 km EASE2 grid and regridded to a quarter degree grid using bilinear interpolation. Pixels with RFI and frozen soil (Holmes et al., 2009) were removed.

5.2.1.1 AMSR-E NN soil moisture

The first AMSR-E soil moisture dataset is developed by Rodriguez-Fernandez et al. (2016) and is determined through the Neural Network approach (AMSR-E NN). Soil moisture from AMSR-E observations is

retrieved using global non-linear relationships which were found by training a neural network to best match the reference soil moisture dataset, in this case SMOS L3 soil moisture. A variety of brightness temperature inputs from AMSR-E were tested, with an optimal input configuration of 6.9 GHz (H/V), 10.7 GHz (H/V), 23.8 GHz (H) and 36.5 GHz (H/V), with the last two frequencies representing information on the soil temperature. This was done for the overlapping time period of SMOS and AMSR-E, from July 2010 to October 2011, and afterwards the optimized neural network was retrospectively applied to the AMSR-E period of 2003 to 2011.

5.2.1.2 AMSR-E REG soil moisture

The second AMSR-E soil moisture data set is developed by Al Yaari et al. (2015), who tested a physically based statistical regression method. SMOS L3 soil moisture is used as a reference to retrieve the regression coefficients that optimally match the AMSR-E 6.9 GHz (H/V) brightness temperatures and soil temperature derived from 36.5 GHz (Holmes et al., 2009) on a point to point base to SMOS L3 soil moisture. Secondly, these regression coefficient where applied to AMSR-E data for the period of 2003 to 2011, to retrieve the AMSR-E REG soil moisture dataset.

5.2.1.3 AMSR-E LPRM soil moisture

The third AMSR-E dataset that is evaluated in this study is developed by Van der Schalie et al. (2017), and uses the physically based Land Parameter Retrieval Model (Owe et al., 2008), which was further developed to specifically allow for the direct integration with SMOS LPRM soil moisture data. The final dataset includes a linear scaling to SMOS LPRM (see section below), bringing the datasets within the same absolute range without changing their individual temporal dynamics. A linear relation for the temperature input from 36.5 GHz observations was established by Holmes et al. (2009). The LPRM was run for the period of 2003 to 2011.

5.2.2 SMOS

The SMOS mission was launched at the end of 2009 by ESA and was the first soil moisture dedicated satellite mission (Kerr et al., 2010; Mecklenburg et al., 2016). The satellite carries the 2D Microwave Imaging Radiometer using Aperture Synthesis (MIRAS) instrument onboard, which observes the Earth's emission at L-band (1.4 GHz), in full polarization and at a wide range of incidence angles (0° - 65°). This frequency is chosen since L-band is theoretically optimal for retrieval soil moisture, with a sensing depth of approximately 5 cm, a higher sensitivity to soil moisture and reduced sensitivity to vegetation cover as compared to higher frequencies (Schmugge, 1983). The spatial resolution ranges between 35 – 50 km, increasing with higher incidence angles. At the equator SMOS has a revisit time of 3 days, with an ascending overpass of around 6 a.m. and a descending overpass around 6 p.m. The ascending data of two SMOS derived soil moisture datasets are used in the evaluation, SMOS Level 3 and SMOS LPRM which are described below. These datasets are provided in a 25 km Equal Area Scalable Earth (EASE) 2 grid and regridded to a quarter degree grid using a standard bilinear interpolation.

5.2.2.1 SMOS Level 3 soil moisture

Two of the fusion approaches, NN and REG, use the Centre Aval de Traitement de Données SMOS Level 3 soil moisture (SMOS L3, v271), which is the official SMOS soil moisture product. The SMOS L3 retrieval algorithm is developed by Wigneron et al. (2007) and Kerr et al. (2012) and is based on solving the radiative transfer model (RTM, Mo et al., 1982), which calculates the emission of a land area, including vegetation cover, for the main land cover in a grid cell and by making use of the multiple incidence angles. Temporally and spatially interpolated soil temperature data from the European Centre for Medium-Range Weather Forecasts (ECMWF) are used for the effective temperature input. Data was used for the period of July 2010 to May 2015. Only data from the SMOS ascending (06:00 AM) overpasses were used in order to have the closest match with the descending (01:30 AM) AMSR-E observations. The SMOS L3 flags were used for filtering,

removing all observations that were flagged with open water, snow, frost, coastal areas or having an RFI probability of over 0.2. The RFI probability is defined in the SMOS L3 product as the total number of observations in which RFI has been detected divided by the total amount of observations in a certain time frame, for which currently a moving average of ± 12 days is used (CATDS, 2014). To minimize the RFI influence to the three merging approaches, a strict boundary of 0.2 was adopted from recent studies (van der Schalie et al., 2016).

5.2.2.2 SMOS LPRM soil moisture

Van der Schalie et al. (2015 & 2016) optimized the Land Parameter Retrieval Model (LPRM, Owe et al., 2008) for SMOS L-band observations which was later updated with a new roughness parameterization and merging strategy (Van der Schalie et al. 2017). This approach was used for the LPRM fusion approach which is in contrast with the others (i.e. NN and REG) that rely on the official SMOS soil moisture product. The LPRM is also based on a radiative transfer model (Mo et al., 1982), however some important points in which the SMOS LPRM distinguishes itself from the SMOS L3 are: 1) the use of a single global parameterization, independent of land cover, 2) the use of an analytical solution for the derivation of the vegetation optical depth (Meesters et al., 2005), and 3) the retrieval is based on the effective average area for soil moisture, instead of for the main land cover (Van der Schalie et al., 2016). For SMOS data flagging, the same procedure is followed for SMOS LPRM as is for SMOS L3. The SMOS LPRM uses only observations with an incidence angle between 35° and 60°, leading to an average decrease in retrievals by 15% compared to SMOS L3. The SMOS LPRM is available for the period of July 2010 to May 2015.

5.2.3 ASCAT soil moisture

The ASCAT soil moisture data product is used as an independent remotely sensed surface soil moisture dataset. Backscatter observations derived from the Advanced Scatterometer (ASCAT) instrument are used to retrieve soil

moisture. ASCAT is a C-band (5.3 GHz) real aperture radar on board two satellites that are part of the Meteorological Operational satellite programme (MetOp-A and MetOp-B), which is a joint program by ESA and the European Organisation for the Exploitation of Meteorological Satellites (EUMETSAT). The MetOp-A satellite was launched in October 2006, with MetOp-B increasing the coverage from September 2012 onwards. The ASCAT soil moisture dataset used in this study was developed by the Technical University in Vienna and is based on the commonly used Change Detection Algorithm (CDA, Wagner et al., 1999; Naeimi et al., 2009). In the CDA, reference backscatters for a vegetated land surface under dry and saturated conditions are used to derive relative soil moisture, presented as a percentage of saturation. The signature of the backscatter over multiple incidence angles is used to correct for inter-annual variations in vegetation cover. The retrievals were done for both ascending (9.30 p.m.) and descending (9.30 a.m.) overpasses, when both overpasses are available their average was taken (Lei et al. 2015). This gives the ASCAT soil moisture dataset a revisit time of 1 to 2 days. Data is used between January 2007 and May 2015.

5.2.4 MERRA soil moisture

Modelled soil moisture from the Modern-Era Retrospective analysis for Research and Applications (MERRA) is used as part of the statistical evaluation strategy (i.e. Triple colocation Analysis (TCA), see Section 5.3.3). MERRA is an atmospheric reanalysis developed by NASA, which uses the Goddard Earth Observing System model, version 5 (GOES-5), supported by the Data Assimilation System (DAS, Rienecker et al., 2008). More specifically, data from the MERRA-Land (Reichle et al., 2011) reanalysis was used, which is specifically developed to improve the output of the model over land and is the recommended dataset for use in hydrological studies over land. These improvements are obtained by two changes over the baseline MERRA model, which is the use of a more accurate precipitation forcing and by using an improved Catchment land surface model. The soil moisture from MERRA-Land as used in this study is the top layer, representing the first 2 cm of the soil. Data is provided in a $^1/_2°$ (latitude) by $^2/_3°$ (longitude) grid, and

regridded using bilinear interpolation to a quarter degree grid. For use in the TCA, it is important to note that the data assimilation system of MERRA-Land does not include satellite retrieved soil moisture, nor passive or active microwave observations.

5.2.5 TRMM 3B42 Precipitation

The R_{value} evaluation requires a precipitation dataset as input. In line with earlier studies, a dataset based on observations from the Tropical Rainfall Measuring Mission (TRMM) is used (e.g. Crow et al., 2010; Parinussa et al., 2011). TRMM was developed in collaboration between NASA and JAXA, with the aim to study precipitation behavior over the tropical regions, and was launched late 1997. Onboard, TRMM carries several rain measuring instruments, the Precipitation Radar, TRMM Microwave Imager and Visible and Infrared Scanner. More specifically, the TRMM 3B42 (v.07) Merged HQ/Infrared Precipitation (Huffman et al., 2007) is used, which provides precipitation rate and precipitation-error estimates between a latitude of 50°N – 50°S. Precipitation estimates from multiple microwave and infrared sensors are used, which are inter-calibrated to TRMM based precipitation estimates, and afterwards a rain gauge based correction was applied. The data was provided in a quarter degree grid and daily files were created by accumulating precipitation over a 24-hour period.

5.2.6 Normalized Difference Vegetation Index (NDVI)

As an indicator for the vegetation, the Normalized Difference Vegetation Index (NDVI) derived from observations by the Moderate Resolution Imaging Spectroradiometer (MODIS) was used. Figure 1 shows the global map of NDVI, including the two hotspots as used in step 4 of the evaluation. MODIS is an instrument on board the Terra and Aqua satellites, and acquires data in 36 spectral bands, ranging from 0.4 μm to 14.4 μm. The NDVI uses infrared and visible observations that are linked to vegetation greenness, which is an indirect measurement for living vegetation and plant chlorophyll content. From MODIS, the monthly NDVI product (MODC13C) was

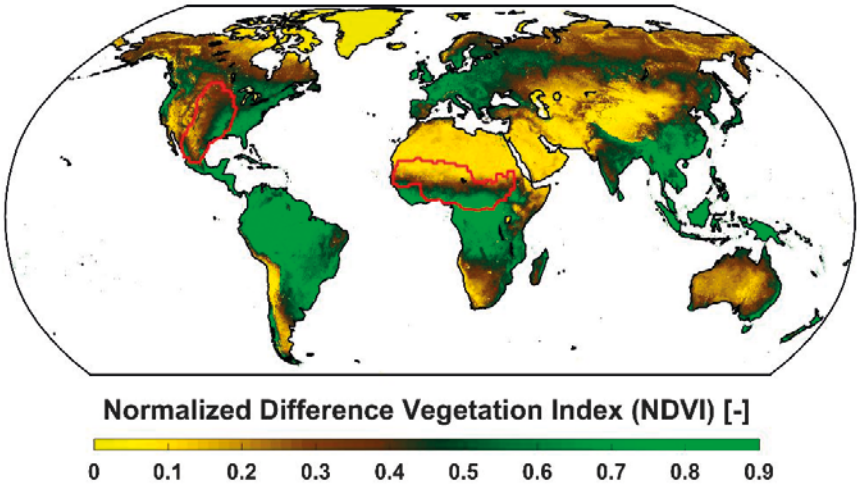

Figure 5.1 Global NDVI values, including the two hotspots used in the TCA and Rvalue evaluation based on Koster et al. (2006), over the Sahel and central Great Plains.

downloaded from which the overall average was taken. The original data was projected on a 0.05° grid which was further aggregated into a global 0.25° grid to match the remotely sensed soil moisture products.

5.3 Methods

5.3.1 Inter-comparison AMSR-E and SMOS soil moisture

The SMOS and AMSR-E retrievals from the three data fusion approaches NN, REG and LPRM are cross-compared during the overlapping period between July 2010 and October 2011. This is done to get a better understanding of the consistency between the different satellites in relation to the different fusion approaches. The Pearson correlation and unbiased root mean square error (*ubrmse*, in $m^3\ m^{-3}$) between the AMSR-E and SMOS datasets were determined, together with their standard deviation (σ). When running statistics for the Pearson correlation, the Fisher z-transformation is applied. These analysis were done over the range of 50°N – 50°S to keep the same

coverage as for the TRMM precipitation dataset as used in the R_{value} evaluation. The *ubrmse* was chosen over *rmse*, since only two of the datasets have either linearly scaled or trained the data on a point to point base (i.e. LPRM and REG), which automatically minimizes the bias.

5.3.2 R_{value} technique

The R_{value} data assimilation approach is based on the connection between precipitation and the subsequent changes in soil moisture (Crow et al., 2010; Parinussa et al., 2011). The technique uses the contrasting quality of two separate rainfall products to evaluate the degree to which analysis increments (derived via the sequential assimilation of soil moisture into a simple water balance model) accurately compensate for known rainfall errors (Crow et al., 2010; Parinussa et al., 2011). More recently, the approach has been adapted to run on an anomaly basis and validated as a robust representation of anomaly-correlation-based skill in satellite soil moisture retrievals (Cow et al., 2010). Here the R_{value} version presented by (Parinussa et al., 2016; Parinussa et al. 2017) is used, that includes the artificial deterioration of the gauge-corrected (3B42) TRMM-based precipitation product instead of relying on its contrast with the near-real-time precipitation dataset. It should be noted that the R_{value} approach has already been successfully applied as a tool for understanding the impact of land cover and sensor characteristics on the quality of satellite-derived soil moisture products (Crow et al., 2010). Furthermore, there are well-known limitations (Parinussa et al., 2011; Parinussa et al., 2016; Parinussa et al., 2017) to the precipitation-based R_{value} verification technique over extremely arid climate regimes, as this technique requires a sufficient number of precipitation events. This requirement cannot be met under extremely arid conditions, as indicated in the figures by “No sensitivity - not enough precipitation”. In line with this limitation of the R_{value} technique is the well-known limitation of remotely sensed algorithms under dense vegetation canopies, as the emission from the soil (moisture) becomes entirely blocked by the overlying vegetation. This limitation in regions with a very dense vegetation cover was indicated in the figures by “No sensitivity - soil moisture looses skills”.

The soil moisture anomalies of the evaluated soil moisture datasets are converted into an antecedent precipitation index (API) and the skill of the API product is tested in the assimilation process for its accuracy to filter out the artificially introduced errors. This level of skill is expressed in the R_{value}, which is based on calculating the Pearson correlation coefficient between the artificially introduced precipitation errors and the Kalman filter analysis increments. Values between 0 and 0.7 are typical for the R_{value} technique, with higher values giving better results (i.e. R_{value} is a performance metrics). Although the exact same spatial cover is taken for all different soil moisture datasets, due to the short overlap time this could not be done temporally. However by taking multiple years (2007-2011 for AMSR-E, 2010-2015 for SMOS and 2007-2015 for ASCAT) and taking the global averages over the NDVI, the influence of the different time period was minimized. For datasets that used the same sensor, only the mutual observations in both space and time were used. More detailed information about this method can be found at Crow et al., 2010 and Parinussa et al., 2011.

5.3.3 Triple Collocation Analysis (TCA)

The triple collocation analysis (TCA) is a statistical verification technique that has been commonly used for the validation of remotely sensed soil moisture anomalies (Dorigo et al., 2010; Parinussa et al. 2011; Draper et al. 2013; Parinussa et al., 2017). The TCA estimates the root mean square error (RMSE) versus true conditions for three linearly related (soil moisture) datasets that have independent error structures. Results from the TCA were validated against ground observations (Miralles et al., 2010) while Dorigo et al. (2010) demonstrated that RMSE estimates are only marginally influenced by the choice of the third product (generally surface soil moisture from a reanalysis model). The conventional product combination in large scale surface soil moisture evaluation studies is soil moisture from an active- and passive microwave source, complemented with the top layer of a reanalysis model. In our case, the active microwave source was chosen to be the ASCAT soil moisture (see 2.3), the reanalysis model was MERRA-Land (see 2.4)

while the passive microwave source was swapped to include the various soil moisture products from retrieved from SMOS and AMSR-E observation. Within this study, we follow the conventional TCA that is extensively documented in literature (Dorigo et al., 2010; Parinussa et al. 2011; Lei et al. 2015; Parinussa et al. 2016; Parinussa et al., 2017). Of specific relevance for the Triple Collocation analysis is the number of collocated samples that was set to at least 100 which is a relatively standard number that was adopted from Parinussa et al. (2011). Additionally, since true soil moisture conditions are unknown, MERRA-Land soil moisture was chosen as reference products but this will not affect subsequent manuscript conclusions regarding the relative performance of all passive microwave products and the product combinations. Triple Collocation produces an error metrics hence higher numbers indicate a lower quality, this in contrast with R_{value} which is a performance metrics.

5.3.4 Results over the regions with strong land-atmosphere coupling

In the final part, the focus is on two major areas that have been recognized as areas with a strong land-atmosphere coupling in the Global Land Atmosphere-Coupling Experiment (GLACE, Koster et al., 2006), which are the Sahel and the central Great Plains of northern America. In the GLACE experiment, twelve different atmospheric general circulation models are evaluated over the boreal summer (June to August) to define common areas with strong coupling in the different models. Two other major areas, which are India and Eastern China, were not further considered in this study due to severe RFI issues in SMOS (e.g. Oliva et al. 2012). The areas identified in the GLACE study are mostly characterized by falling in a transition zone between humid and arid climates. In order to affect large atmospheric processes, two requirements need to be met, first the evapotranspiration must be sensitive to soil moisture, and secondly there must be a high temporal variability in evapotranspiration (Koster et al., 2006). For very arid climates, this is not met due to the sparse moments that enough soil moisture is available to affect large scale atmospheric processes, while for humid areas there is almost always plentiful soil moisture available for evapotranspiration. The transition zones however, does meet these two

requirements. This arid to humid pattern is also reflected in the vegetation cover (Figure 5.1), as arid climates are mostly covered by sparse vegetation which increases to dense tropical rainforests in the humid regions. In this evaluation, both the TCA and R_{value} results are compared and visualized over these regions.

5.4 Results and discussion

5.4.1 Inter-comparison AMSR-E and SMOS soil moisture

Figure 5.2 shows the results for the inter-comparison of the three fusion methods, i.e. for AMSR-E against SMOS LPRM (LPRM, ▬), AMSR-E NN against SMOS L3 (NN, ▬) and AMSR-E REG against SMOS L3 (REG, ▬). Figure 5.2A presents the correlations versus the average annual NDVI. Overall, the NN ▬ approach gives the highest correlations between SMOS and AMSR-E soil moisture with temporal correlation coefficients above 0.7 for NDVI values under 0.7. The other two fusion datasets (LPRM ▬ and REG ▬) reveal slightly lower correlations, but very similar to each other, having temporal correlation coefficients above 0.7 for NDVI values under 0.6. REG ▬ shows higher correlations than LPRM ▬ for very low (<0.15) values, while LPRM ▬ has slightly higher correlations between an NDVI of 0.15 and 0.6. The difference between NN ▬ and the other two approaches increases with increasing vegetation. When looking at the σ of the correlation, a clear opposite trend was demonstrated. The σ of the correlation is low when the mean correlation is high, and when the mean correlation is decreases (e.g. with denser vegetation), the variation as seen in the σ increases. This correlation analysis reveals that from the three different approaches, the NN ▬ has the highest consistency between the two frequencies.

A glance at Figure 5.2C, which shows the *ubrmse* between the AMSR-E and SMOS soil moisture products, reveals a slightly different outcome than the temporal correlation coefficients. Here, the variation of the *ubrmse* over different vegetation regimes is quite similar for all three approaches. NN and REG have the lowest *ubrmse* up to an NDVI of 0.2. Then all three approaches

have similar *ubrmse* variation for the NDVI range between 0.2 and 0.4. Over the more densely vegetation areas (NDVI > 0.4), LPRM and NN give the lowest *ubrmse*. Differences however are very small, with an *ubrmse* between 0.02 and 0.04 m^3 m^{-3} for NDVI values below 0.6. The σ of the *ubrmse* reveals a similar behavior as for the mean *ubrmse*, it steadily increases with denser vegetation up to an NDVI of 0.65, with values ranging between 0.005 and 0.020. This shows that all three fusion methods are well able to closely match the soil moisture dynamics of the two datasets.

These results give us confidence that both the soil moisture products of the different satellite sensors have similar behavior over the low and moderately vegetated areas (i.e. between the NDVI regime of 0.2 and 0.6). For the sparse (i.e. NDVI < 0.2) and densely vegetated regions (NDVI > 0.6) the soil moisture retrievals from the different satellite sensors show a reduced consistency. These findings are in line with previous work (e.g. Al-Yaari et al., 2014; Holgate et al., 2016; Van der Schalie et al., 2017) and is most likely related to the differences in frequencies between the two sensors. At C-band the vegetation attenuation is stronger than at L-band which results in a lower accuracy over more vegetated regions (Al-Yaari et al., 2014).

Figure 5.3 shows the distribution of sample sizes (N) that are used within the NDVI binning procedure in this study. Between an NDVI range of 0.15 and 0.65, the used points per bin are between 30 and 60% of the total possible points over our quasi-global study area. For regions with NDVI values under 0.15, still >500 points remain per bin but becomes a smaller fraction of the total, while for an NDVI > 0.65 the total used points decreases quickly. This caused by an insufficient amount of precipitation

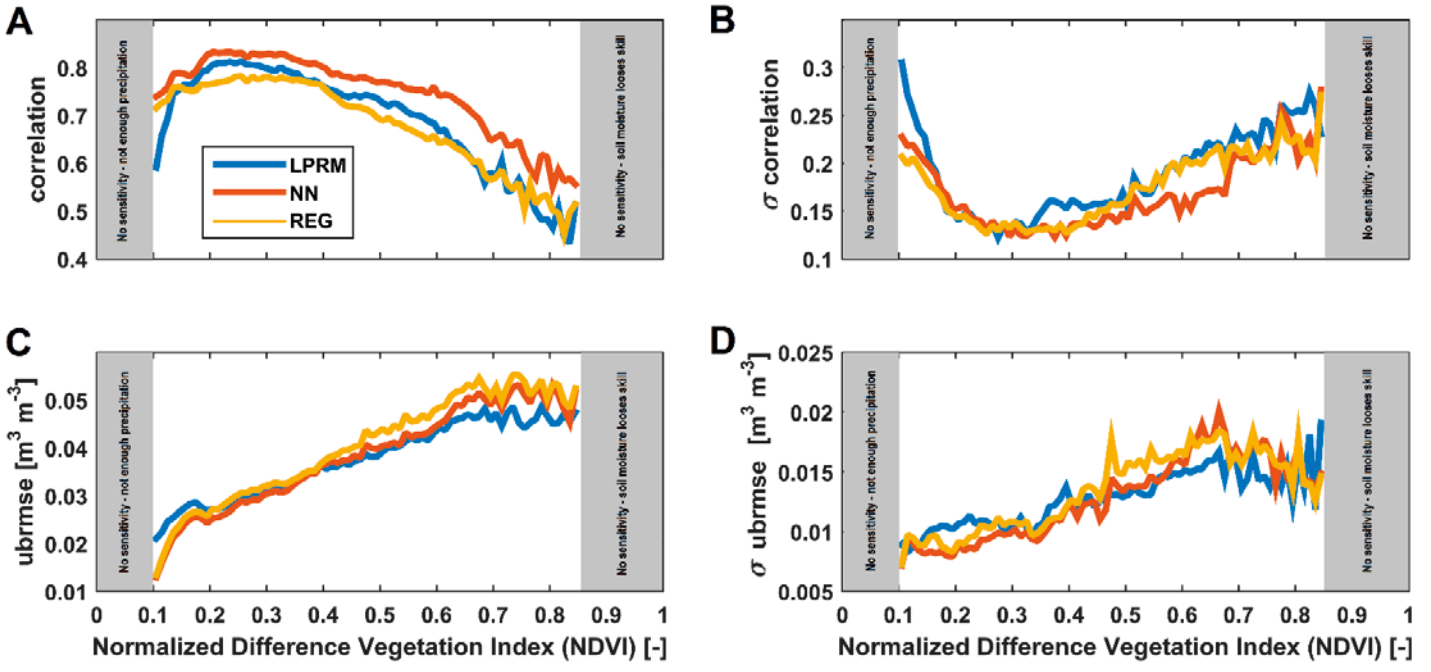

Figure 5.2 Inter-comparison of the three different fusion methods of AMSR-E against SMOS, in terms of correlation (A), standard deviation of the correlation (B) ubrmse (C) and standard deviation of the ubrmse (D) binned over NDVI.

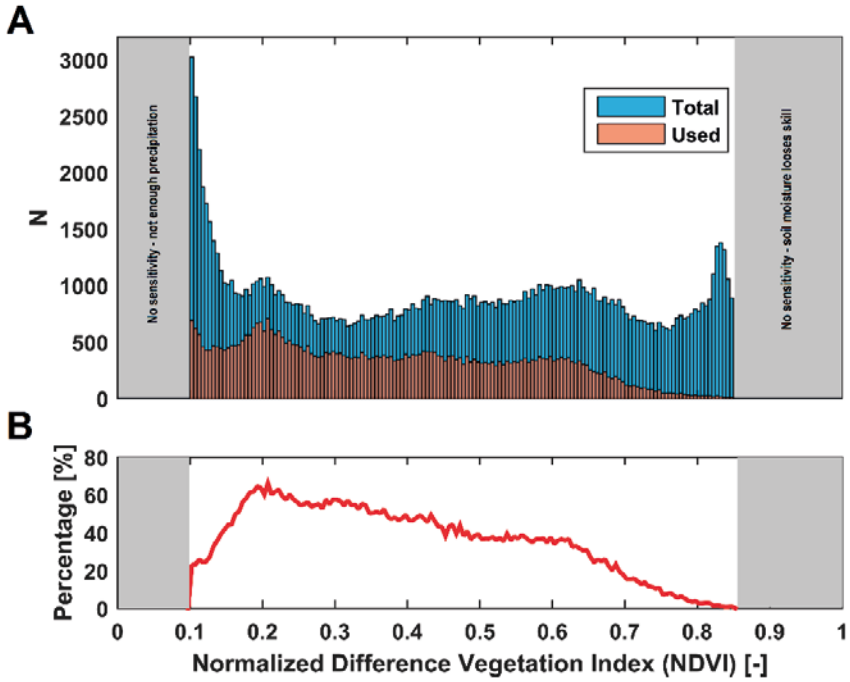

Figure 5.3 Number of points used in the evaluation compared to the total amount of points available over our quasi-global study area, divided in NDVI bins with steps of 0.005 (A), and the percentage of the used data points within the NDVI binning procedure as compared to the total points (B).

events for the R_{value} approach (Section 5.3.2 and 5.4.2) in the NDVI < 0.15 region. Secondly, the small amount of retrievals over dense forest in the SMOS LPRM dataset leads to reduced availability in the NDVI>0.65 bins. Over the evaluated NDVI range, RFI occurrence in either L-, C- or X-band are removed, leading to the removal of almost all of Eurasia due to L-band RFI (e.g. Oliva et al. 2012).

5.4.2 R_{value} technique

In Figure 5.4 the binned results of the precipitation based R_{value} verification technique are shown which provide information on the anomaly based correlation skills of the individual datasets. The R_{value} of the different AMSR-E retrievals vary over the sparse to moderate vegetated domain (i.e. NDVI 0.1 – 0.4) and beyond an NDVI value of 0.4 they all decline from around 0.5 to values below 0.3 at an NDVI of 0.85. AMSR-E LPRM ▬ has the overall highest values for the low vegetated regions, with $R_{value} > 0.5$. At NDVI levels of 0.6 and beyond AMSR-E NN ▬ demonstrates higher R_{value} compared to AMSR-E LPRM ▬. AMSR-E REG ▬ has the lowest values compared to the other AMSR-E products (i.e. NN and LPRM). The two SMOS products (i.e. SMOS L3 ▬ and SMOS LPRM ▬) demonstrate a similar performance throughout with a slightly better performance for SMOS LPRM between an NDVI of 0.3 and 0.6. At NDVI values between 0.35 and 0.55 the SMOS products produce the highest R_{value} compared to all other products. Beyond NDVI values of 0.55 the ASCAT ▬ retrievals demonstrate the best performance reflected by the highest R_{value} beyond that NDVI threshold. These findings are generally in line with previous studies by De Jeu et al. (2008) and Dorigo et al. (2014) and clearly demonstrate how different products can complement each other.

The lower R_{value} of AMSR-E NN and AMSR-E REG over the sparsely vegetated regions (i.e. NDVI < 0.35) as compared to AMRS-E LPRM might be explained by the fusion strategies, as the NN and REG approach are bound by the training set of SMOS L3. This might result in a slightly decreased performance compared to SMOS L3, and a dependency on the performance of SMOS L3, e.g. over the more sparsely vegetated area. This is the area where the physical based model LPRM might have an advantage. However, more research is needed to fully understand the reasoning of the difference between the AMSR-E products over this vegetation regime. The R_{value} of the linear REG approach drops quickly with increasing vegetation (NDVI > 0.4), while still showing a good performance over the lower vegetated area. The NN provides lower values in these sparse vegetated areas, while keeping a stable performance over denser vegetation, and producing the highest

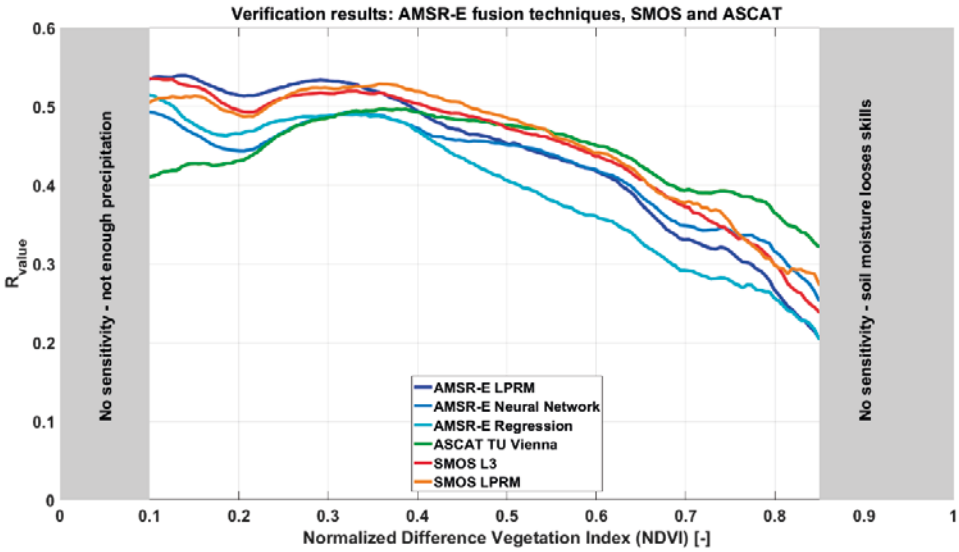

Figure 5.4 R_{value} results binned over NDVI for all 6 satellite soil moisture datasets, based on three different fusion techniques and three microwave sensors.

values at high NDVI values over 0.6, which is most likely caused by making optimal use of the multi frequency AMSR-E input and L-band training dataset.

5.4.3 Triple Collocation Analysis (TCA)

Figure 5.5 shows the results of the second evaluation technique, the TCA, as identically binned compared to the R_{value} . It should again be noted that the R_{value} is a performance metrics hence higher numbers indicate a better performance while TCA produces an error metrics hence lower numbers indicate a better performance. In contrast with the presented R_{value} results in which we generally focused on the highest numbers, we now generally focus on the smallest errors. These TCA results generally confirm the findings obtained by the R_{value} technique (section 5.4.2), however, small differences

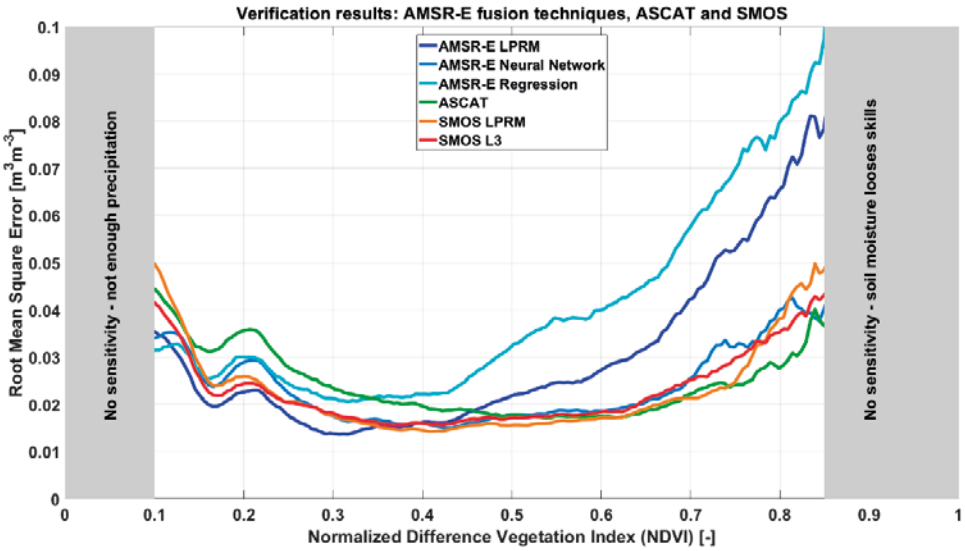

Figure 5.5 TCA results binned over NDVI for all 6 satellite soil moisture datasets., based on three different fusion techniques and three microwave sensors

were demonstrated too. Again, AMSR-E LPRM ▬ shows the lowest *rmse* values within the lower NDVI range (NDVI<0.4), then the SMOS products (i.e. SMOS L3 ▬ and SMOS LPRM ▬) again take over and demonstrate the best performance indicated by the lowest *rmse* values. Again, at more densely vegetated regions, the ASCAT ▬ soil moisture anomalies demonstrate the best performance which is indicated by the lowest *rmse*. It should also be noted that for the NDVI range between 0.4 and 0.7, the AMSR-E NN ▬, SMOS L3 ▬, SMOS LPRM ▬ and ASCAT ▬ *rmse* generally demonstrate a similar performance. For SMOS, the performance of the two datasets have a similar crossover point in performance as with the R_{value} technique.

Even though the L-band observations are theoretically more sensitive to changes in soil moisture, the higher frequency observations from AMSR-E

are performing better over the more sparsely vegetated areas. Al-Yaari et al. (2014) also found this difference but the reason for this is still unknown. It might be due to the difference of the radiometric accuracy of AMSR-E (<1 K) versus the radiometric accuracy of SMOS (2-4 K), which could play a role over regions where vegetation attenuation has a smaller impact than the direct signal to noise ratio performance. For example, a sparse vegetated region could create a range of 100 K for L-band and 80 K for C-band when you vary from saturated to dry conditions, while for more vegetated regions this range will significantly drop at C-band down to only 5 K, where L band is still producing a range of 40 K. Another plausible solution might be related to the complexity to estimate effective temperature, Parinussa et al. (2011) showed that in (semi-) arid climate regions effective temperature derived from simultaneous Ka-band observations specifically adds information compared to extracting this effective temperature input from reanalysis models which is currently being done for both SMOS soil moisture products.

5.4.4 Results over two regions with a strong land-atmosphere coupling

From a climate perspective the regions where soil moisture has a strong coupling with the atmosphere have the highest interest. Here the focus will be put on the largest areas. The first area covers the central Great Plains of northern America, and the second the Sahel region. The results of the R_{value} and TCA for the six individual soil moisture datasets are shown in Figure 5.6 (the central Great Plains) and Figure 5.7 (the Sahel).

For the central Great Plains all datasets mainly reach R_{value} values between 0.4 and 0.7. The two SMOS datasets, L3 and LPRM, have comparable values and patterns, with the R_{value} hardly dropping below 0.5 and showing the highest overall values. The AMSR-E datasets do show a slight drop in skill over the Eastern areas to values of 0.4, where the vegetation density increases, but reaches the highest values in the western part. When comparing the three AMSR-E sets, very similar patterns can be found, with

AMSR-E LPRM giving the highest values, followed by AMSR-E REG and AMSR-E NN. ASCAT is showing high values in the central part of the Great plains but it's performance significantly drops in the Chihuahuan Desert which is characterized by extremely arid conditions.

The TCA results over the central Great plains are shown in Figure 5.6G to L. Here, both the SMOS datasets show the lowest overall *rmse* values, with little differences between the two SMOS products (i.e. LPRM and L3). The influence of the vegetation on the quality of the soil moisture products can be seen in both AMSR-E and SMOS datasets, with AMSR-E significantly increasing in *rmse* over the more dense vegetation. For the AMSR-E datasets, the AMSR-E NN dataset has the lowest overall *rmse*, followed by AMSR-E LPRM and to a lesser extent AMSR-E REG. ASCAT gives mainly average *rmse* values between 0.02 and 0.03 $m^3\ m^{-3}$. For the TCA, results were masked over the Chihuahuan Desert (Figure 5.6L to G), as the TCA as it does not meet the standard TCA requirements over that area (Scipal et al. 2008).

The second area that was analyzed in more detail is the Sahel region, of which the results of the R_{value} and TCA are shown in Figure 5.7. In the R_{value} results, a clear split can be seen between the north-western and south-eastern part of the region. The highest values for the north-western part are found for the AMSR-E LPRM dataset, reaching high R_{value} of >0.5 for the complete area, this is followed by AMSR-E REG, AMSR-E NN, SMOS L3 and SMOS LPRM, which keep values of >0.4 for the whole region, and finally ASCAT, which has the lowest values over this semi-arid region. In the south-eastern part, covered with denser vegetation, the highest R_{value} are found for the SMOS L3 dataset, still reaching values beyond 0.4 in many cases. This is followed by SMOS LPRM, ASCAT, AMSR-E NN, AMSR-E LPRM and low values <0.2 are found for AMSR-E REG.

The results from TCA over the Sahel are less clear. Here four datasets showing a good performance with mainly *rmse* < 0.025 $m^3\ m^{-3}$, which are the

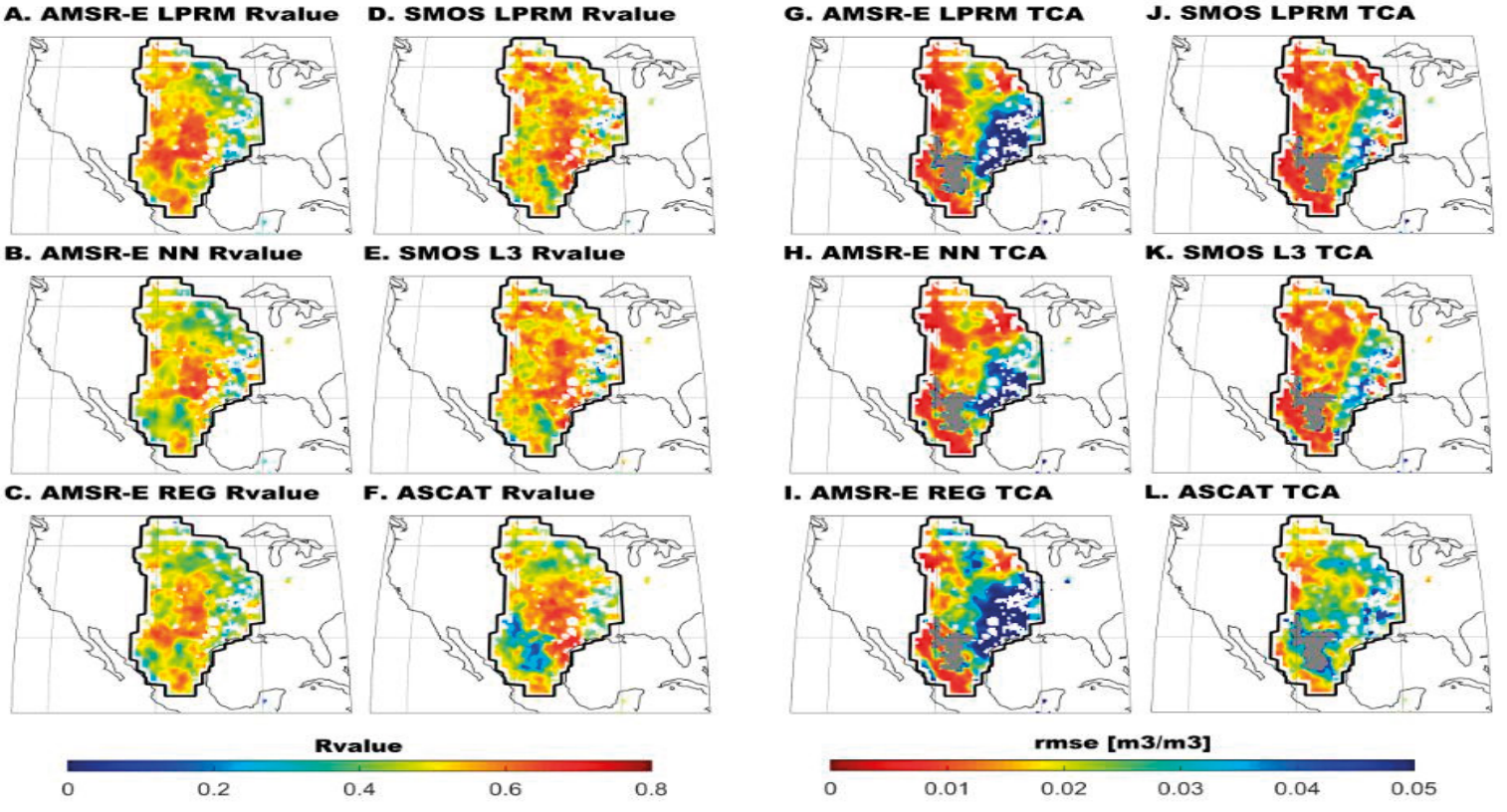

Figure 5.6 R_{value} (A to F) and TCA (G to L) results over the central Great Plains of northern America. The Chihuahuan Desert is masked out (gray) in the TCA results.

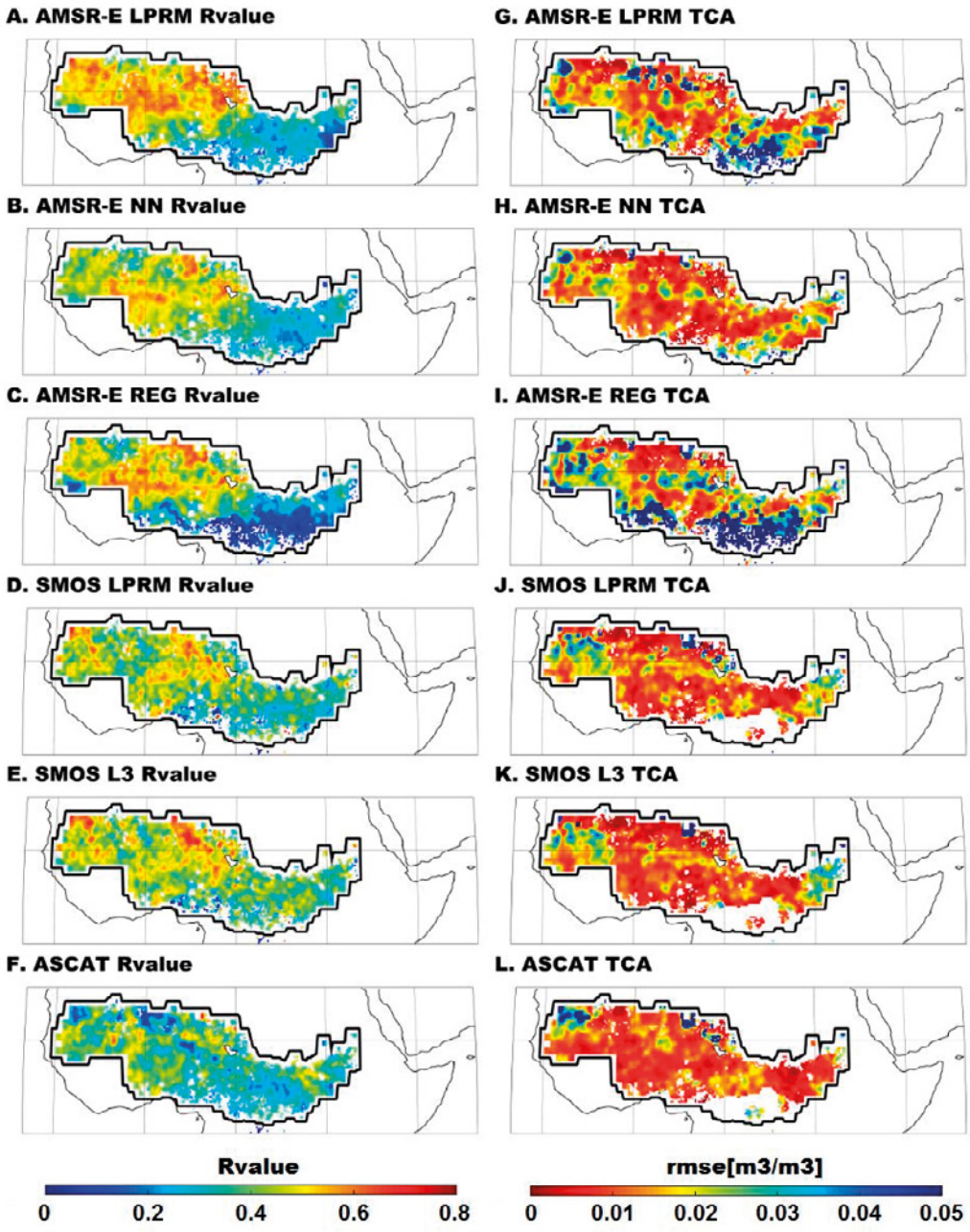

Figure 5.7 R_{value} (A to F) and TCA (G to L) results over the Sahel.

ASCAT, SMOS L3, SMOS LPRM and AMSR-E NN. The AMSR-E LPRM and AMSR-E REG show several areas where the *rmse* is higher than 0.04 m^3 m^{-3}. In the southern part this reflects the area with denser vegetation and is in line with what was seen in the R_{value} patterns, however in the more northern parts, where AMSR-E LPRM and AMSR-REG performed best when looking at the R_{value}, several of those areas also appear.

The findings over the Sahel and central Great Plains reflect the results from the earlier sections in this study. The AMSR-E datasets, especially AMSR-E LPRM, are able to provide high quality soil moisture datasets over the low to moderate vegetated areas and both SMOS datasets are extending the quality more towards moderate to dense vegetated areas, while ASCAT shows a reasonable performance over the whole range, being less affected by vegetation variations, with the exception of the dry/semi-arid areas. These findings are in line with an earlier study over the Continental United States (Lei et al. 2015) that also used the TCA that was verified through ground based soil moisture observations. This study shows that current the evaluated soil moisture datasets are well able to provide high quality soil moisture in regions with strong land-atmosphere interactions.

5.5 Conclusion

As the availability of consistent long term soil moisture records is of increased importance to climate researchers, this study evaluates the quality of three different merging strategies that have been specifically developed to combine soil moisture retrievals from multiple satellite sensors. In this case on soil moisture retrievals based on AMSR-E and SMOS observations, putting extra focus on the integration of L-band based soil moisture in such a data record. Three approaches were evaluated which differ in the way that (1) is based on applying a global neural network to retrieve SMOS L3 like soil moisture from AMSR-E observations (NN), (2) is based on applying local regressions to AMSR-E observations to best match SMOS L3 soil moisture (REG), and (3) applies the physically based Land Parameter Retrieval Model

to SMOS observations and updates its parameterization for improved AMSR-E based retrievals (LPRM).

First, a global inter-comparison exercise was done to quantify the consistency between the SMOS and AMSR-E based soil moisture retrievals in terms of correlation and *ubrmse*, i.e. for AMSR-E LPRM against SMOS LPRM (LPRM), AMSR-E NN against SMOS L3 (NN) and AMSR-E REG against SMOS L3 (REG). When evaluating the correlations, the NN approach reaches the highest values over the complete vegetation range, having average correlations of over 0.7 up to an NDVI of 0.7, which is higher than the REG and LPRM approaches, which drop below that point at an NDVI of 0.6. The *ubrmse* shows an increasing trend with denser vegetation, from 0.02 $m^3\ m^{-3}$ up to 0.05 $m^3\ m^{-3}$, and varies little between the three methods. This shows that AMSR-E and SMOS register similar behavior in soil moisture over the low and moderately vegetated areas.

Secondly the quality of the individual datasets to detect soil moisture was evaluated using two different evaluation techniques, the precipitation based R_{value} technique and the Triple Collocation Analysis (TCA), including ASCAT to cover the active counterpart of satellite based soil moisture retrievals. The results from the R_{value} technique show the strength of using the three different data sources. AMSR-E LPRM soil moisture performed best over areas with an NDVI of up to 0.35, followed by the two SMOS datasets (LPRM and L3). The SMOS datasets perform slightly better over areas with an NDVI between 0.35 and 0.55, with first AMSR-E LPRM and with denser vegetation ASCAT following closely. In the highest NDVI regions, ASCAT shows the highest performance, followed by the SMOS datasets. This combination of sources manages to keep high R_{value} between 0.55 and 0.4 up to an NDVI of 0.75, slowly decreasing with denser vegetation.

The TCA shows many similarities to the results as found from applying the R_{value} technique, keeping a low *rmse* in areas up to an NDVI of 0.80. Again

AMSR-E LPRM shows the best performance, i.e. lowest *rmse*, in areas with an NDVI up to 0.35. After that, several datasets show same level of performance, with first between an NDVI of 0.35 and 0.45 the AMSR-E NN, AMSR-E LPRM, SMOS LPRM and SMOS L3 datasets, and for higher values the AMSR-E NN, SMOS LPRM, SMOS L3 and ASCAT datasets. In the areas with denser vegetation, the SMOS and ASCAT based retrievals show very similar results.

In the last section two specific regions with a land-atmosphere coupling, the Sahel and the central Great Plains of northern America, were evaluated in more detail. The findings here mainly reflect results that are found in earlier section. While SMOS L-band observations are theoretically more sensitive to soil moisture, the AMSR-E observations are still performing better over the more sparsely vegetated areas, probably caused by the higher radiometric sensitivity of the instrument and the possibility to use observation driven temperature. Spatial consistency in soil moisture records can be improved with L-band measurements due to the stable performance of SMOS over the whole range of NDVI values. These results also show that the currently available satellite based soil moisture datasets, based on both passive (e.g. AMSR-E and SMOS) and active microwave observations (e.g. ASCAT), are well able to provide a valuable source of information over a wide range of vegetation regimes when combined in an optimal way.

5.6 Acknowledgement

This project is supported by the ESA project "Passive Microwave Soil Moisture Data Fusion Study" (Contract # 4000110112). Further funder by ESA was provided under ESAs Climate Change Initiative Program ”Phase 2 of the ESA Climate Change Initiative – Soil Moisture ECV” , contract no. 4000112226/14/I-NB).